Figures Calculus III

Felix Claeys, Brecht Verbeken, Simon Verbruggen

October 12, 2025

1.2.3 Example evolute cycloid

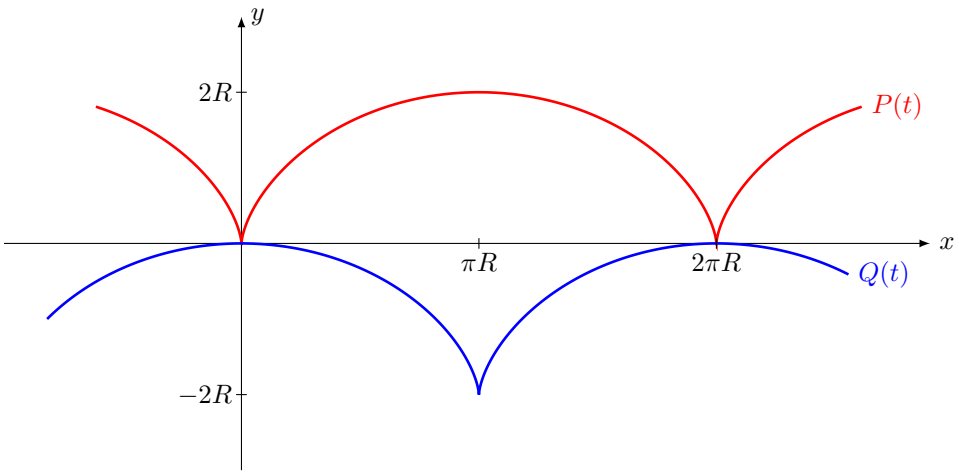

Figure 1: The cycloid $P(t) = [R(t - \sin t), R(1 - \cos t)]$ and its evolute $Q(t) = [R(t + \sin t), R(\cos t - 1)]$, which is a translation of $P(t)$.

1.2.4 Example evolute catenary

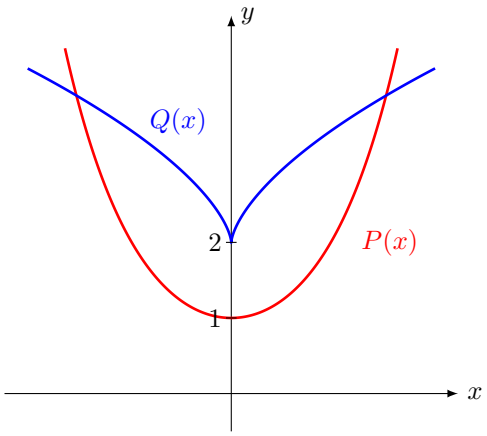

Figure 2: The catenary $P(x) = [x, a\cosh(x/a)]$ and its evolute $Q(x) = \left[x - \frac{a}{2}\sinh(2x/a), 2a\cosh(x/a)\right]$.

1.2.5 Example involute catenary (tractrix)

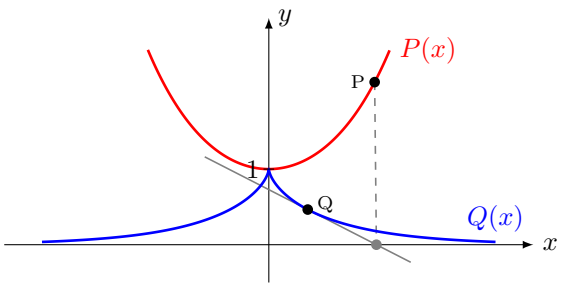

Figure 3: The catenary $P(x) = [x, a\cosh(x/a)]$ and its involute: the tractrix $Q(x) = \left[x - a\tanh(x/a), \frac{a}{\cosh(x/a)}\right]$. For a point Q on the tractrix, the intersection of the tangent to Q with the X-axis coincides with the orthogonal projection of the corresponding point on the catenary P.

1.2.8 Example envelope family of straight lines

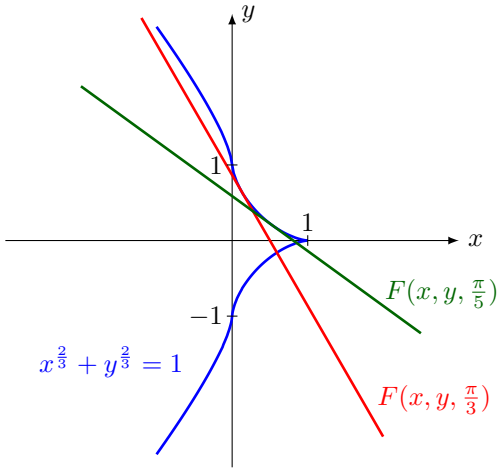

Figure 4: Some examples from the family of lines $F(x, y, a) = \frac{x}{\cos(a)} + \frac{y}{\sin(a)} = 1$, and the corresponding astroid: $x^{2/3} + y^{2/3} = 1$.

2.3 Gradient of scalar field

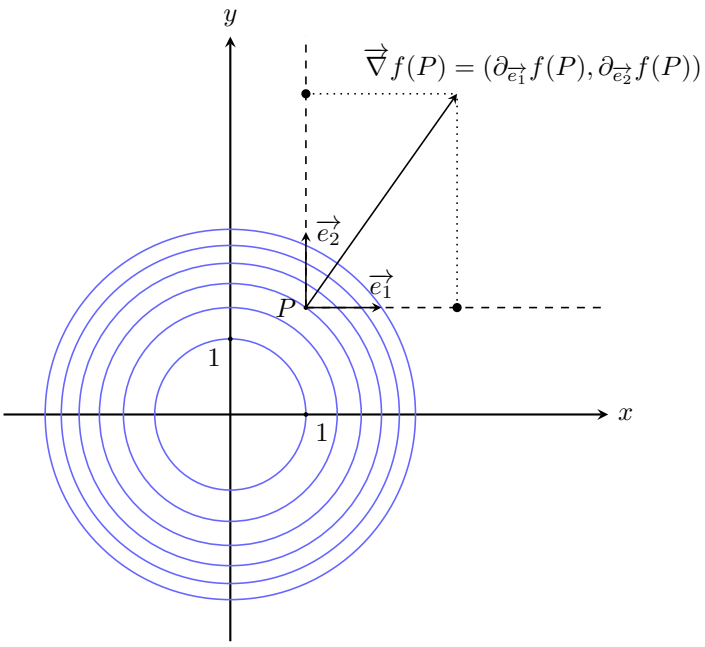

Figure 5: The scalar field $f(x, y) = x^2 + y^2$ visualized by the planes $f(x, y) = n$ for $n \in \{1, 2, 3, 4, 5, 6\}$. The gradient $\vec{\nabla} f(P)$ in a point P is given with its directional derivatives $\partial_i f(P) = \partial_{\vec{e}_i} f(P)$.

3.1 Line integral of a scalar field

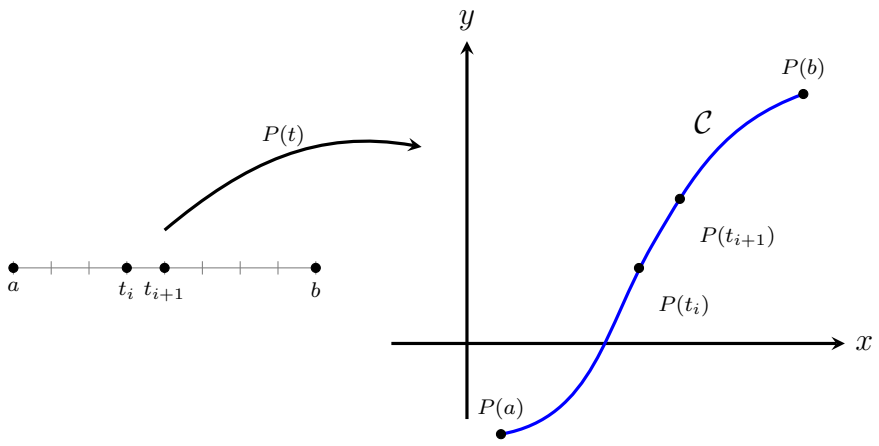

Figure 6: The line integral of a scalar field ϕ over a smooth curve $P(t)$ is given by: $\int_{\mathcal{C}} \phi \; ds := \int_a^b \phi\left(P(t)\right) \left\| \frac{\overrightarrow{dP}}{dt} \right\| dt$. In the figure, the displacement between different points along the curve, $P(t_{i+1}) - P(t_i)$, is shown. This relates to the infinitesimal displacement $\left\| \frac{\overrightarrow{dP}}{dt} \right\| dt$.

3.2 Line integral of a vector field

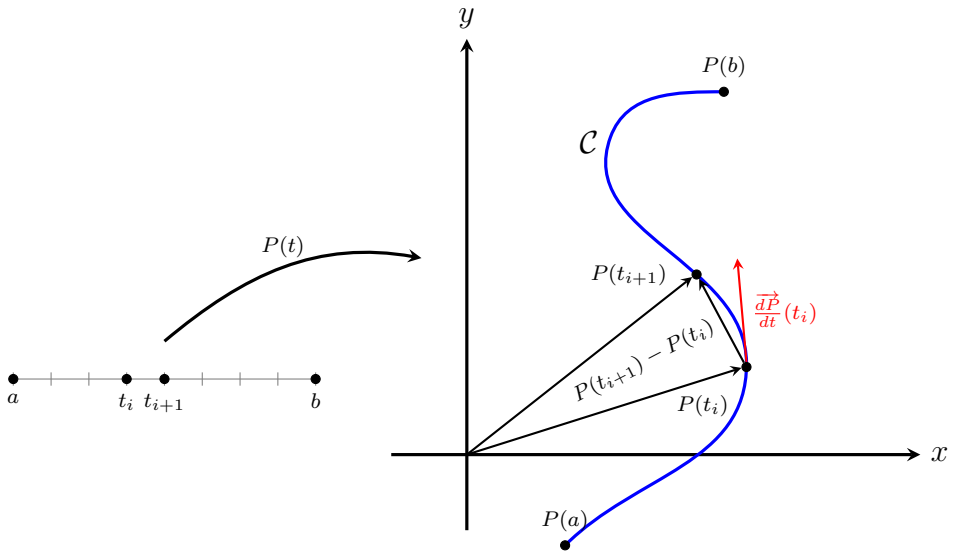

Figure 7: The line integral of a vector field $\overrightarrow{F}$ over a smooth curve $P(t)$ is given by: $\int_{\mathcal{C}} \overrightarrow{F} \cdot \overrightarrow{dP} := \int_a^b \overrightarrow{F}\left(P(t)\right) \cdot \frac{\overrightarrow{dP}}{dt}\, dt$. In the figure, the displacement between different points along the curve, $P(t_{i+1}) - P(t_i)$, is shown. This relates to the infinitesimal displacement vector $\frac{\overrightarrow{dP}}{dt} dt$.

3.4.2 Conservative field along a curve

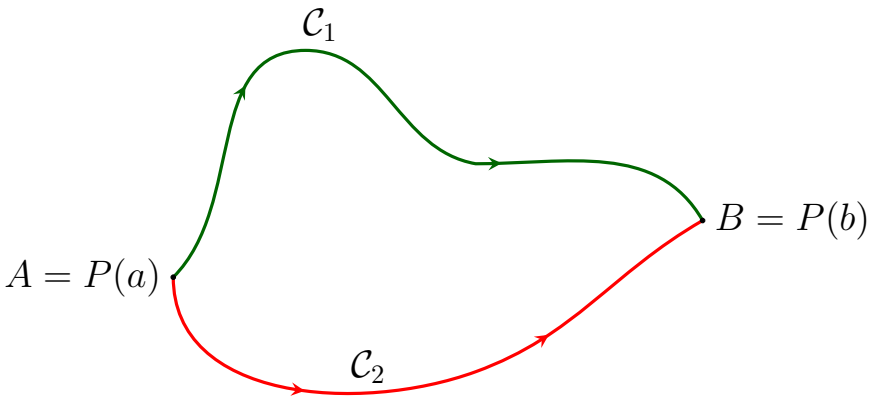

Figure 8: The points A and B lie on a closed curve $\mathcal{C}$. We can choose two arbitrary paths, $\mathcal{C}_1$ and $\mathcal{C}_2$, from A to B. If we evaluate the line integral of a conservative field ϕ along both paths, the result will be the same, since the line integral of a conservative field is independent of the travelled path.

3.4.3 Proof conservative field

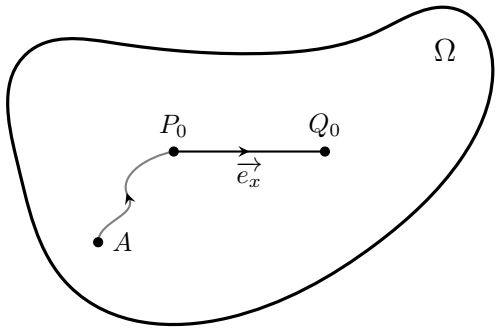

Figure 9: Proof that path-independence implies conservativeness in fields. Consider a path-independent vector field $\vec{F}$ in an open, connected region Ω. A potential function $\phi(P_0)$ is constructed by integrating $\vec{F}$ along an arbitrary curve $\widehat{AP_0}$ from a fixed point A to P_0. The path independence ensures that ϕ is well-defined, and its gradient reproduces $\vec{F}$.

3.5.1 Proof Greens theorem

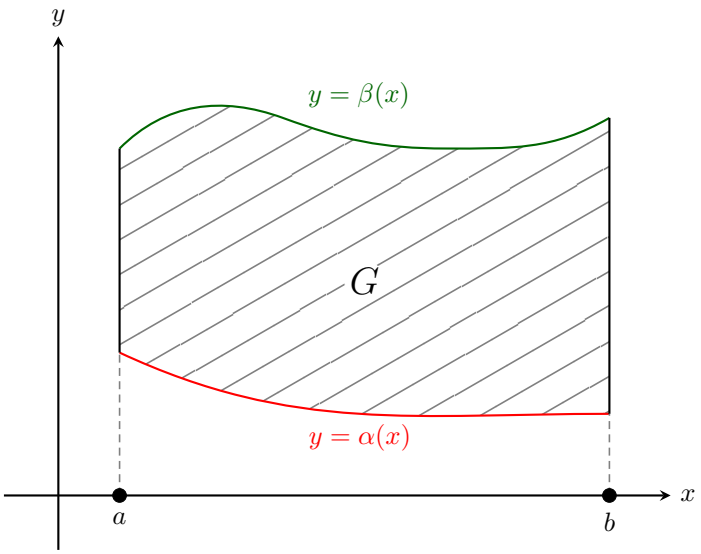

Figure 10: The normal region G can be projected onto the x-axis, with its upper and lower boundaries parametrized by $y = \alpha(x)$ and $y = \beta(x)$.

3.5.2 Union of normal spaces

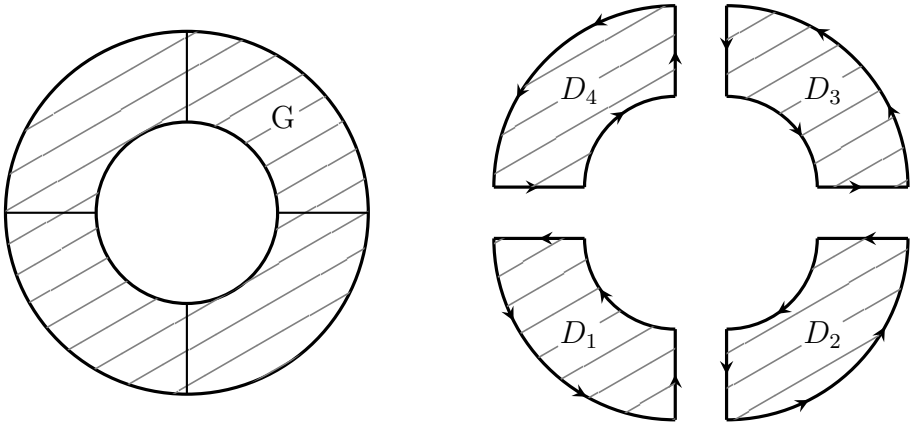

Figure 11: (Left) The annulus G is not a normal region, as it cannot be projected onto the X- or Y-axis. (Right) However, G is a union of normal regions: it can be split into four regions (D_i) each of which can be projected onto the X- and Y-axis.

3.5.4 Alternative formulation Greens theorem

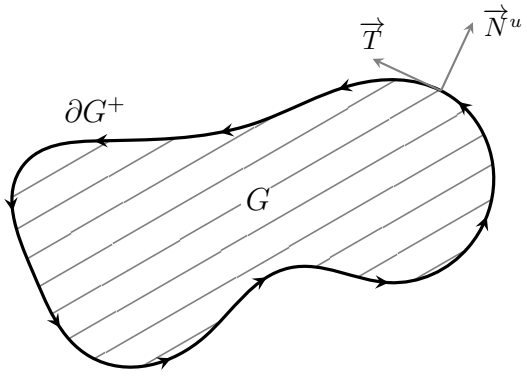

Figure 12: The alternative representation of Green's theorem: $\int_{\partial G^+} \overrightarrow{F} \cdot \overrightarrow{N}^u \, ds = \int_G \overrightarrow{\nabla} \cdot \overrightarrow{F} \, dA$, where $\overrightarrow{T}$ is the tangent unit vector and $\overrightarrow{N}^u$ the outward normal vector.

4.1 Surface integral of a scalar field

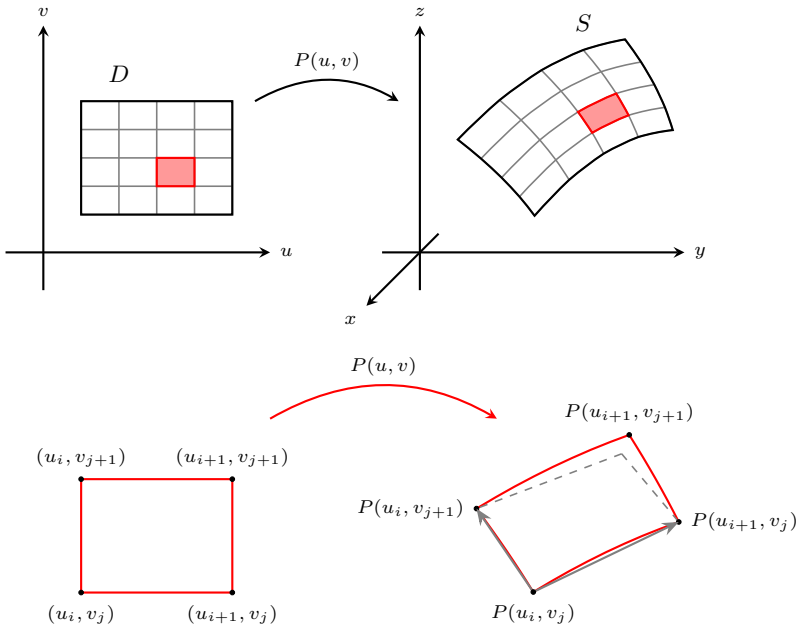

Figure 13: Construction of the surface integral of a scalar field ϕ over a smooth surface $S = P(u, v)$: $\int_S \phi \; d\sigma := \int_D \phi\,(P(u,v))\, \|\overrightarrow{\partial_u P} \times \overrightarrow{\partial_v P}\| \; du \; dv$ (Below) An infinitesimal rectangle on D with area $du_i \; dv_j$ is projected onto a curvilinear quadrilateral on S, which we can approximate by a parallelogram, with area: $|(P(u_{i+1}, v_j) - P(u_i, v_j))\,(P(u_i, v_{j+1}) - P(u_i, v_j))\,| = \|\overrightarrow{\partial_u P(u_i, v_j)} \times \overrightarrow{\partial_v P(u_i, v_j)}\| \; du_i \; dv_j$. This is represented in the integral by the absolute value of the Jacobian determinant associated with the parameterization: $\|\overrightarrow{\partial_u P} \times \overrightarrow{\partial_v P}\|$.

4.4.1 The divergence theorem

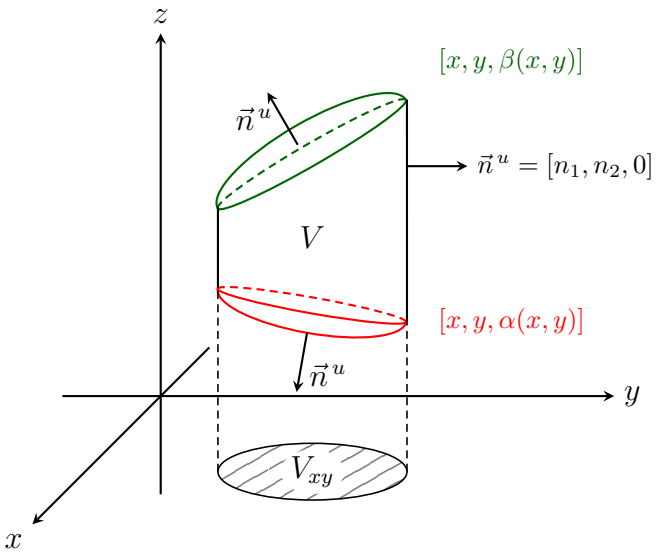

Figure 14: Proof of the divergence theorem. The normal region V is projected onto the XY-plane, with projection V_{xy}. The upper and lower boundaries of V are represented by a parametrization.

4.6.0 The corkscrew rule

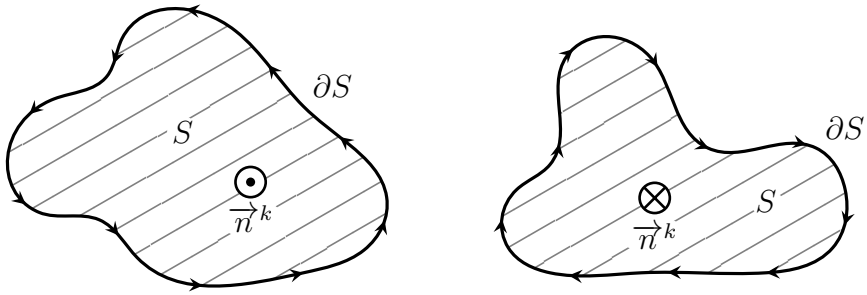

Figure 15: The unit vector along the surface normal, $\overrightarrow{n}^k$, is oriented such that its direction agrees with the orientation of ∂S according to the corkscrew rule (or right-hand rule).

4.6.1 Stokes theorem

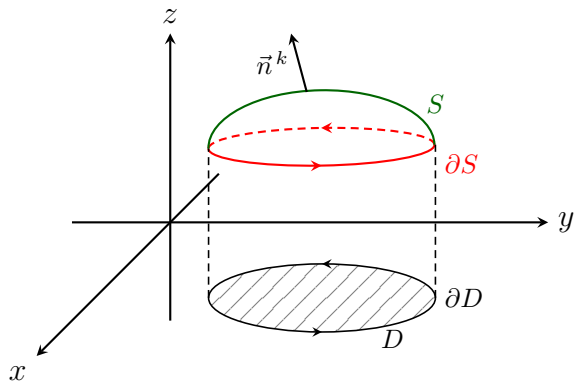

Figure 16: Proof Stokes' theorem. S is a smooth surface that can be projected onto the XY-plane, with projection D.

5.1 Inverse function

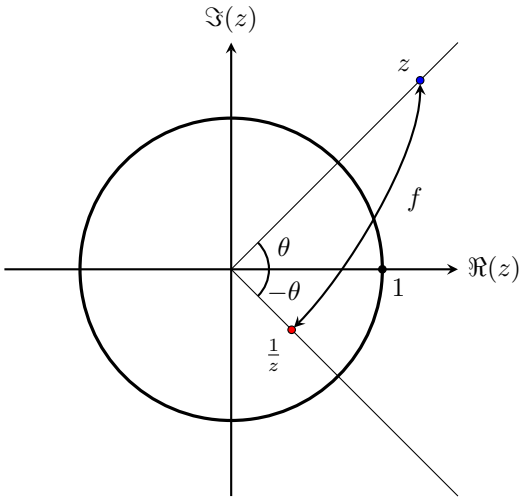

Figure 17: The reciprocal function $f(z) = \frac{1}{z}$ maps points outside of the unit circle inside the unit circle and vice versa. The ray with an angle θ will be mapped to a ray with angle $-\theta$.

5.1 Complex function

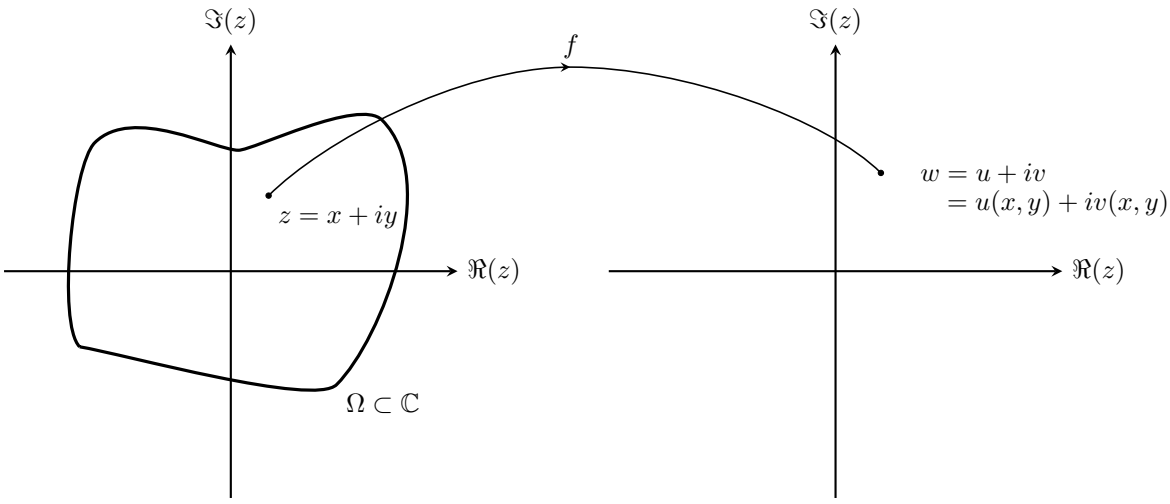

Figure 18: The complex function $f : \Omega \to \mathbb{C}$ which maps points from $\Omega \subseteq \mathbb{C}$.

5.2 Complex line integral

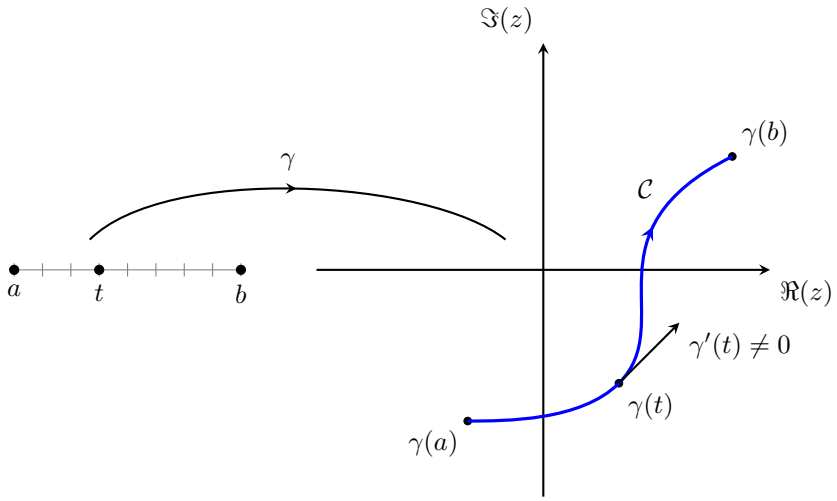

Figure 19: The complex line integral $\int_C f(z)\,dz$ for $z = \gamma(t)$, $t \in [a, b]$, with $\gamma(t)$ a smooth curve, can also be seen as an integral over t with the equation $\int_C f(z)\,dz = \int_a^b f(\gamma(t))\,\gamma'(t)\,dt$

6.2.1 Complex derivative

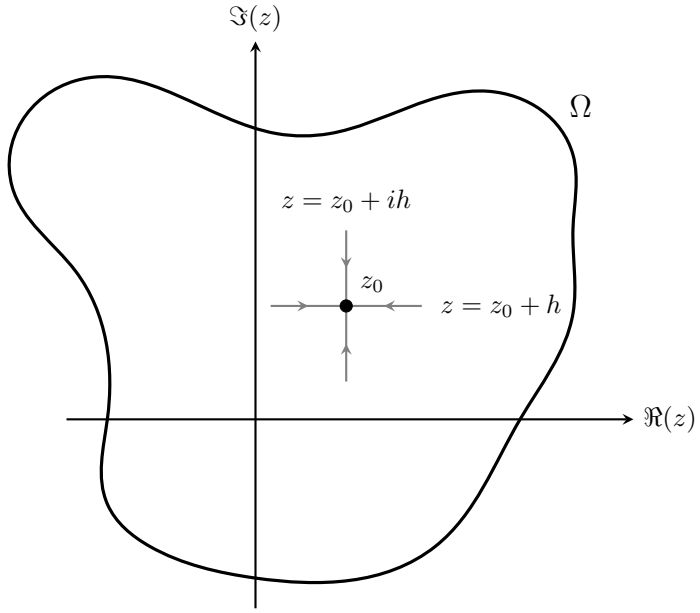

Figure 20: The complex derivative in a point $z_0 = x_0 + iy_0$ for a complex function is: $f'(z_0) = \lim_{h \to 0} \frac{f(z_0+h)-f(z_0)}{h}$. For $f'(z_0)$ to exist, this limit must be the same regardless of the direction in which $h \to 0$. In the figure, the limit is approached along the real and imaginary axes; equating the results of both approaches yields the Cauchy–Riemann conditions.

6.3 Cauchy Goursat theorem for multiply connected domains

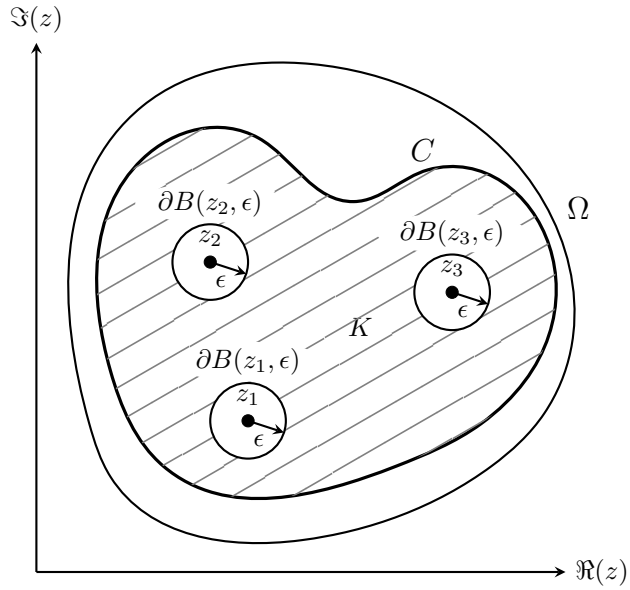

Figure 21: The integral over a contour C in Ω with an interior with a finite amount of singular poles is the sum of the integrals over the circles around these interior poles.

6.3 Contour non simply connected

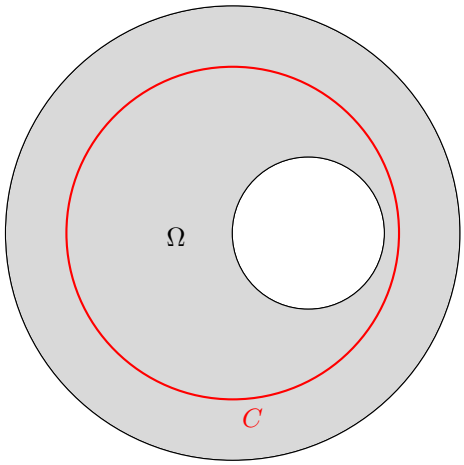

Figure 22: The interior region of C does not lie entirely within Ω. Wherefore we need information about the set of points not in Ω.

6.3 Contour simply connected

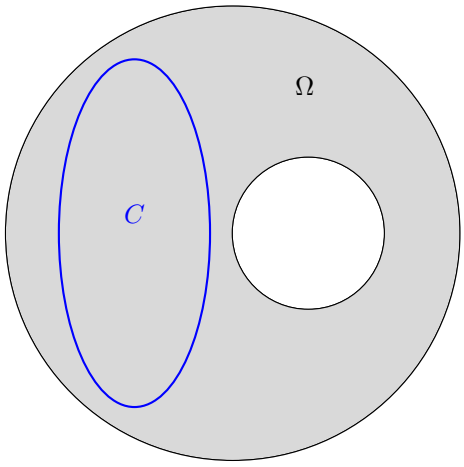

Figure 23: C encloses a compact set that lies entirely within Ω. In this case, the integral over the contour will be zero.

6.3.3 Proof integral formula Cauchy

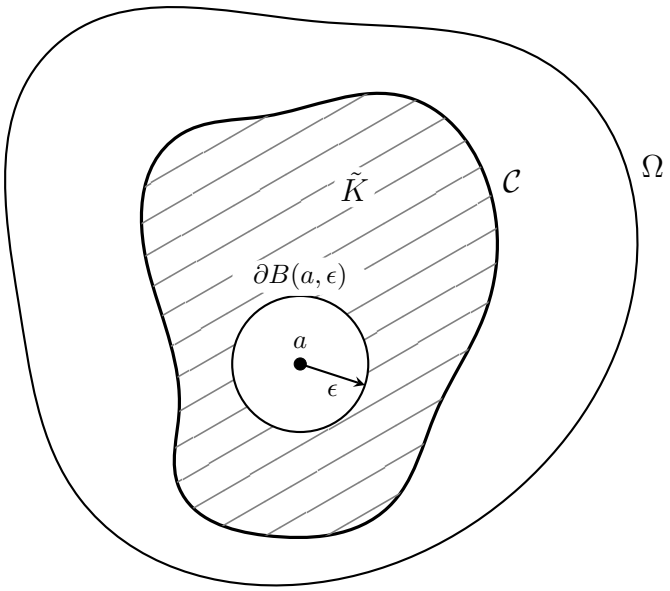

Figure 24: $\mathcal{C}$ is a bounded contour in Ω which encloses a compact set K lying completely within Ω. For a point $a \in \mathcal{C} \setminus K$, we parametrize the circle $\partial B(a, \epsilon)$, which lies entirely in the interior of $\mathcal{C}$.

7.2.4 Theorem convergence regions positive and negative power series

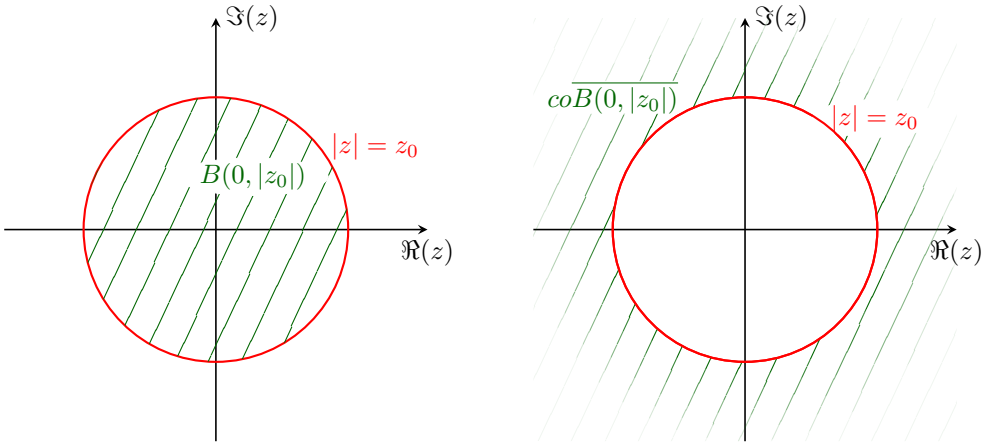

Figure 25: (Left) Region of convergence of a positive power series. (Right) Region of convergence of a negative power series.

8.2.1 Proof theorem Laurent series

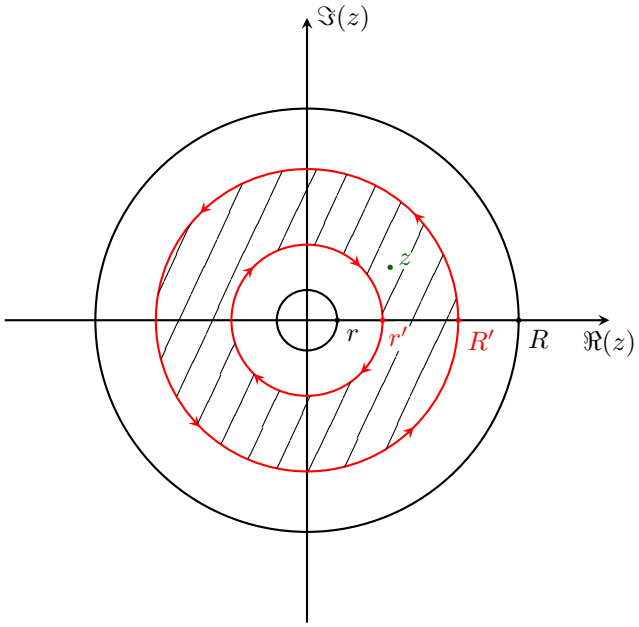

Figure 26: The region of convergence of the Laurent series is the annular region $B(0,R) \setminus \overline{B(0,r)}$. For every point z, it is possible to find R' and r' such that $0 < r < r' < |z| < R' < R$.

8.5.6 Residue theorem for region with multiple singularities

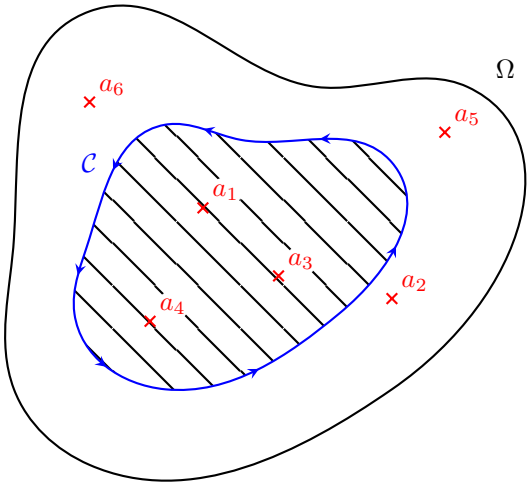

Figure 27: The contour $\mathcal{C}$ passes through none of the singularities a_i of the complex function f and encloses a compact set that lies entirely within Ω. $\mathcal{C}$ contains a finite number of singularities of f.

9.3 Estimation lemmas

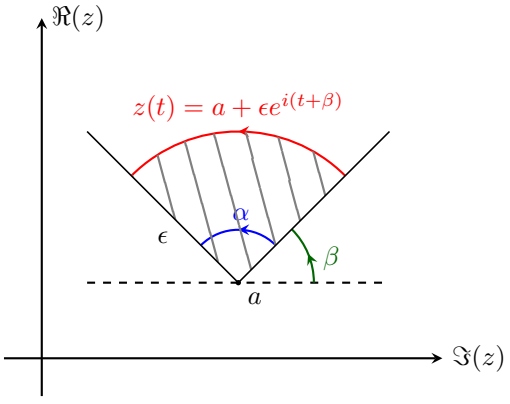

Figure 28: Small limit theorem: The circular arc C_ε^t with center a, radius $\varepsilon > 0$, and central angle α can be described by the parametric equation $z(t) = a + \varepsilon e^{i(t+\beta)}$, $t : 0 \to \alpha$.

9.5 Summation of series

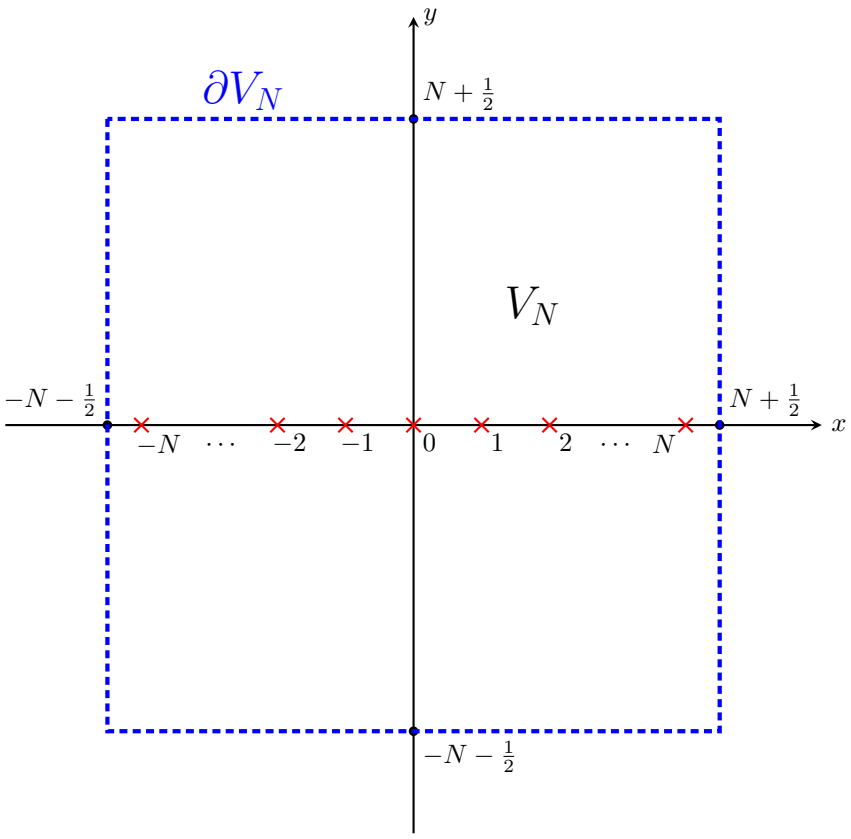

Figure 29: The function $g(z) = \cot(\pi z)$ has simple poles at $z = 0, \pm 1, \pm 2, \ldots$. If we consider the square V_N with center at the origin and side length $2N+1$, where $N \in \mathbb{N}$, then we can compute the contour integral over ∂V_N^+ using the residue theorem.